



# Influence of natural convection on beam propagation in fluidic optical device



Byunggi Kim\*, Hong Duc Doan, Kazuyoshi Fushinobu

Department of Mechanical and Control Engineering, Tokyo Institute of Technology, Mail Box I6-3, Ookayama 2-12-1, Meguro-ku 152-8552, Japan

## ARTICLE INFO

### Article history:

Received 21 April 2015

Received in revised form 4 June 2015

Accepted 27 June 2015

### Keywords:

Thermal lens effect

Fluidic optical device

Natural convection

Beam propagation method

Beam shaping

## ABSTRACT

The fluidic optical device by means of the thermal lens effect has attracted increasing attention as a flexible beam shaper. However, onset of natural convection inhibits operation of the fluidic optical device as it causes asymmetric distortion on shaped beam profile. For implementation of the fluidic beam shaper, this adverse effect should be controlled in terms of the beam profile change. From this perspective, we investigated the influence of natural convection on the propagating beam profile through the fluidic optical device by means of CW laser induced the thermal lens effect. Numerical method taking advantage of beam propagation method was used to calculate modulation of the probe beam profile. The calculated results demonstrated good agreements with several experimental results. Using this numerical model, the parametric study to control asymmetry and quality of the annular beam was performed quantitatively in the dual beam thermal lens system. The core of this study is that the solution of the simple pentadiagonal equation can provide the crucial investigation on the modulation of the beam profile in the fluidic optical device with natural convection.

© 2015 Elsevier Ltd. All rights reserved.

## 1. Introduction

After Gordon et al. [1] reported the transient and defocusing thermal lens effect of liquid, the thermal lens spectroscopy has been used for measurement of material properties with small absorbance. Several researchers [2–5] used the thermal lens spectroscopy to investigate linear thermo-optic properties using CW laser. Also, extensive studies [6–10] have been carried out to describe nonlinear optics of liquid using short and ultra-short pulsed lasers. With the progress of those works, the thermal lens effect has been understood in detail to derive many helpful theoretical models describing the thermal lens phenomena and modulation of the beam. In addition to these measurement researches, change of the beam profile itself is also of interest recently. Taking advantage of the thermal lens effect, we have developed the fluidic optical device as a flexible beam shaper [11–13]. One major characteristic of the fluidic optical device is that it can be used for both spatial and temporal laser beam shaping. Doan et al. [11,12] demonstrated the principle of the spatial beam shaper by means of the thermal lens effect and an application to Bessel beam generation system. In their study, it was confirmed that various beam profile could be easily obtained by controlling pump

beam power. On the other hand, Kim et al. [13] reported temporal pulse-shaping technology of nanosecond-pulsed laser. From the result that pulse compression of 21.7% was achieved by their experiment, it was indicated that the thermal lens spectrometry can be applied for new oscillation mechanism of short-pulsed laser.

In those works, the thermal lens effect is utilized with various pump lasers for individual applications. The formation of the refractive index field significantly depends on optical parameters (such as CW or pulse, pulse width, power, beam waist, and configuration of absorbing sample). In particular, parameters such as pump beam power can be easily controlled without any change of the optical devices in many systems. Therefore, the fluidic optical devices have excellent flexibility as a beam shaper.

However, local absorption and heating inevitably results in large temperature gradient. Therefore, natural convection may occur in liquid medium and the convective flow brings out the distortion of the temperature field and refractive index field around the beam propagation axis. It leads to asymmetry of the beam spatial profile around the optical axis. Consequently, natural convection has an adverse effect on quality of the shaped beam. Akhmanov et al. [14] first investigated the thermal self-actions of laser beam, and several other works [15–17] provide theoretical studies on the onset of convection in transient regime. Most recently, Karimzadeh [17] demonstrated theoretical approach to

\* Corresponding author. Tel.: +81 3 5734 2500.

E-mail address: [kim.b.aa@m.titech.ac.jp](mailto:kim.b.aa@m.titech.ac.jp) (B. Kim).

## Nomenclature

$\mathbf{v}$	flow velocity, $(u, v, w)$ , m/s	$w_0$	$1/e^2$ pump beam radius at focus, m
$\rho$	density, $\text{kg}/\text{m}^3$	$\lambda_p$	wavelength of probe beam, m
$p$	pressure, Pa	$R_0$	$1/e^2$ original probe beam radius, m
$\eta$	viscosity, $\text{kg}/(\text{s m})$	$W$	$1/e^2$ probe beam radius, m
$\beta$	thermal expansion coefficient, $1/\text{K}$	$W_0$	$1/e^2$ probe beam radius at focus, m
$T$	temperature, K	$n$	refractive index
$g$	gravity acceleration, $\text{m}/\text{s}^2$	$n_0$	refractive index at $T_0$
$c_p$	specific heat, $\text{J}/(\text{kg K})$	$E$	electric field, $\text{N}/\text{C}$
$\kappa$	thermal conductivity, $\text{W}/(\text{m K})$	$\hat{i}$	unit vector
$h$	heat transfer coefficient, $\text{W}/(\text{m}^2 \text{K})$	$j$	imaginary unit
$S$	source term, $\text{W}/\text{m}^3$	$k_0$	free space wave number, $\text{m}^{-1}$
$\alpha$	absorption coefficient, $1/\text{m}$	$I$	intensity, $\text{W}/\text{m}^2$
$x, y, z$	coordinates, m	$L$	cuvette thickness
$P_0$	pump beam irradiation power, W	$f$	focal length of the lens
$\lambda_e$	wavelength of pump beam, m	$z_R$	Rayleigh length, m
$r_0$	$1/e^2$ original pump beam radius, m	$M^2$	beam quality factor
$w$	$1/e^2$ pump beam radius, m		

study transient self-phase modulation of a CW laser beam using Fresnel–Kirchhoff diffraction integral in the approximation of an optically thin absorbing medium. However, there are few reports on the behavior of propagating beam using numerical method. It must be conducted to evaluate quality of shaped beam profile with accuracy, in order to investigate the influence of natural convection for design of fluidic optical devices.

The objective of this study is to theoretically investigate and evaluate modulation of the beam profile through convective field in CW induced thermal lens system. In Section 2, the numerical approach to describe development of natural convection and the probe beam propagation are explained. In Section 3, experimental setup is represented to investigate modulation of the beam profile in the single beam system. In Section 4, experimental and theoretical results are demonstrated, and parametric study on quality of the shaped beam profile is conducted theoretically in the dual beam thermal lens system. The discussion will focus on modulation and distortion of annular-like profile, which attracts increasing attention for various applications [12,18,19].

## 2. Theory

### 2.1. Thermal lens system

Separation of the pump and probe beams is usually taken into account in order to obtain large change of the probe beam signal and flexibility on the thermal lens system. For the CW thermal lens system, refractive index change is predominated by temperature change. The probe beam experiences significant defocusing as liquid normally has negative value of  $dn/dT$  [8]. Schematic illustration of the thermal lens system used in this study is shown in Fig. 1. The ethanol-dye solution is used as a liquid sample because its  $dn/dT$  is large enough to conduct significant beam shaping. The beams parallel to ground are irradiated into the sample set parallel to the direction of the gravitational acceleration. The sample is filled in the glass cuvette with optical thickness  $L$ . Temperature field around optical axis is distorted upon the direction of the gravitational acceleration so that symmetry of the beam profile is also lost.

We used the Cartesian coordinates. The optical axis was set as  $z$  coordinates, and the direction of gravitational acceleration was matched with  $y$  direction.

### 2.2. Development of natural convection

Since temperature increase induced by CW laser absorption is only few several degrees of Kelvin, Boussinesq approximation can be used in the present context. The liquid sample and two walls of glass cuvette were set as calculation region as shown in Fig. 2. The calculation region on  $x$ - $y$  plain was selected as  $5 \text{ mm} \times 5 \text{ mm}$  size square around the beam at the center as shown in Fig. 2(a) (size of the liquid sample on  $x$ - $y$  plain:  $24 \text{ mm} \times 30 \text{ mm}$ ). Thickness of glass cell was  $1.5 \text{ mm}$  (therefore calculating length on the  $z$ -direction was  $4 \text{ mm}$ , Fig. 2(b)). The governing equations are written as followings:

$$\nabla \cdot \mathbf{v} = \mathbf{0} \quad (1)$$

$$\rho(\mathbf{v} \cdot \nabla)\mathbf{v} = -\nabla p + \eta \nabla^2 \mathbf{v} - \rho \beta(T - T_0)\mathbf{g} \quad (2)$$

$$\rho c_p(\mathbf{v} \cdot \nabla)T = k \nabla^2 T + S \quad (3)$$

Eqs. (1)–(3) show the continuity equation, the conservation of momentum equation, and conservation of energy equation respectively. The glass wall was considered as no-slip wall, and the interface between the glass wall and ambient air was set as the natural convection boundary condition with  $5 \text{ W}/\text{m}^2$  heat transfer coefficient. Also, as calculation region on  $x$ - $y$  plain was selected around the beam, temperature boundary condition was set on four cross sections as  $T = T_0$  as represented in Fig. 2(a). As the calculation region is large enough compared to beam radius, this temperature boundary condition can be applied to improve calculation performance.

Here, heating induced by CW laser is given as a source term  $S$  in Eq. (3). Considering Lambert–Beer law on propagating direction and the Gaussian intensity distribution,  $S$  can be written as following equation when the focal point of the beam is in the cuvette.

$$S = \alpha \exp(-\alpha z) \times \frac{2P_0}{\pi w_0^2} \exp\left[-2 \frac{(x^2 + y^2)}{w_0^2}\right] \quad (4)$$

The source term,  $S$ , is expressed as a product of absorbing term and spatial intensity profile term. In fact, because the pump beam is focused, the beam radius and the intensity distribution of the beam vary in the cuvette. However, we did not reflect these axial effects because of the following reasons. First, as the cuvette thickness is very small ( $L = 1 \text{ mm}$ ) compared to the focal depth of the beam ( $116 \text{ mm}$ ), change of the beam radius in the cuvette is ignorable.

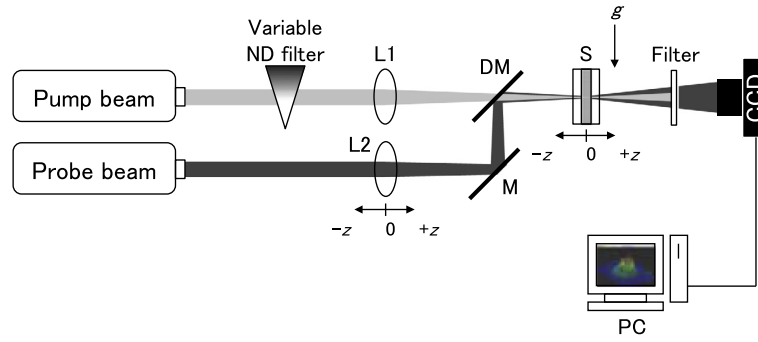


**Fig. 1.** Schematic illustration of the dual beam thermal lens system: Natural convection in the cuvette leads to asymmetry of the transmitted beam profiles. It depends significantly on optical parameters of the system.

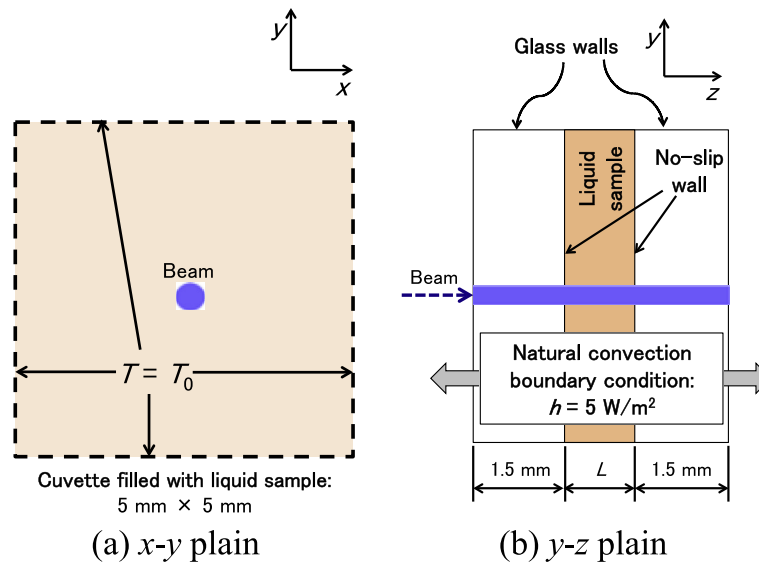


**Fig. 2.** Calculation region and boundary conditions: (a)  $x$ - $y$  region was selected as  $5\text{ mm} \times 5\text{ mm}$  size around the beam at the center. Temperature boundary condition was set on cut cross sections. (b) Glass walls were considered as no-slip wall. Natural convection boundary condition was considered at the interface between the cuvette and ambient air.

Furthermore, as absorption coefficient ( $\alpha = 1.65\text{ cm}^{-1}$ ) and the pump beam power ( $P_0 = 2.0\text{--}14.0\text{ mW}$ ) are also very small in the present context, change of the intensity distribution of the pump beam in the cuvette is not significant and can be neglected. The value of  $S$  is 0 other than the liquid because absorption coefficient of glass is assumed 0.

Eqs. (1)–(4) are solved by using ANSYS 15.0 Fluent. The second order upwind scheme are applied for spatial discretization. We used the thermal properties of the ethanol (Table 1) instead of the ethanol-dye solution whereas the experimental and calculation results would not perfectly match.

In the case that the irradiation direction is parallel to the gravitational acceleration, the effect of buoyancy can be ignored as the

cuvette thickness is small. Therefore, the solution without second term of right hand side of Eq. (2) gives the temperature field without natural convection.

### 2.3. Refractive index field

Note that variation of refractive index in medium heavily depends on temperature change. This relation is written as following simple linear equation:

$$n = n_0 + \Delta T \frac{dn}{dT} \tag{5}$$

Since temperature field is given, and  $dn/dT$  is determined uniquely as a property of liquid, refractive index field can be easily found by Eq. (5).

### 2.4. Beam propagation

The numerical solution utilizing Padé approximant operators is employed to calculate intensity distribution of the propagating beam. This numerical solution covers strong focusing or defocusing effects on Cartesian coordinate system. The derivation of the equations used in the numerical solution starts from the following

**Table 1**  
Thermal properties of the ethanol at 300 K [20].

Parameter	Unit	Value
Refractive index of the ethanol		1.36
Refractive index change, $dn/dT$	$\times 10^{-4}\text{ K}^{-1}$	3.6 [8]
Density, $\rho$	$\text{kg/m}^3$	783.5
Viscosity, $\eta$	$\text{mPa s}$	1.045
Coefficient of thermal expansion, $\beta$	$\text{mK}^{-1}$	1.073
Specific heat, $c_p$	$\text{kJ}/(\text{kg K})$	2.451
Thermal conductivity, $k$	$\text{mW}/(\text{m K})$	166

vector wave equation, which describes change of electric field of the propagating beam:

$$\nabla^2 E(x, y, t) - \frac{1}{c^2} E(x, y, t) = 0 \quad (6)$$

With the assumption that behavior of vector field can be treated as scalar quantities, the separation of variables is used to describe electric field as a scalar field [21]:

$$E(x, y, t) = \hat{i}\varepsilon(x, y) \exp(-j\omega t) \quad (7)$$

In addition, a plane wave assumption simplifies the wave equation with the following solution of form:

$$\varepsilon(x, y, z) = \Psi(x, y, z) \exp(-jk_0 n_0 z) \quad (8)$$

Consequently, by substituting Eqs. (7) and (8) into Eq. (6), the scalar wave equation is derived without the time dependence:

$$-\frac{\partial^2 \Psi}{\partial z^2} + 2jk_0 n_0 \frac{\partial \Psi}{\partial z} = \frac{\partial^2 \Psi}{\partial x^2} + \frac{\partial^2 \Psi}{\partial y^2} + k_0^2 [n^2(x, y, z) - n_0^2] \Psi \quad (9)$$

The Padé method rearranges Eq. (9) into the recursive form using (1, 1) order Padé approximant operator [22]:

$$\frac{\partial \Psi}{\partial z} = -\frac{\frac{j\hat{P}}{2k_0 n_0} \Psi}{1 + \frac{\hat{P}}{4k_0^2 n_0^2}} \quad (10)$$

where

$$\hat{P} = \left[ \frac{\partial^2}{\partial x^2} + \frac{\partial^2}{\partial y^2} + k_0^2 [n^2(x, y, z) - n_0^2] \right] \quad (10.1)$$

Using Crank–Nicolson method as a finite difference approximation to the derivatives, above Eq. (10) can be rearranged to the pentadiagonal form of equation:

$$\begin{aligned} & \delta(-) \left[ \Psi_{ix-1, iy}^{iz} + \Psi_{ix+1, iy}^{iz} + \Psi_{ix, iy-1}^{iz} + \Psi_{ix, iy+1}^{iz} \right] \\ & + \left[ \gamma \delta(-) + 4k_0^2 n_0^2 \Delta x \Delta y \right] \Psi_{ix, iy}^{iz} \\ & = \delta(+)^{-1} \left[ \Psi_{ix-1, iy}^{iz+1} + \Psi_{ix+1, iy}^{iz+1} + \Psi_{ix, iy-1}^{iz+1} + \Psi_{ix, iy+1}^{iz+1} \right] \\ & + \left[ \gamma \delta(+)^{-1} + 4k_0^2 n_0^2 \Delta x \Delta y \right] \Psi_{ix, iy}^{iz+1} \end{aligned} \quad (11)$$

where

$$\delta(\mp) = 1 \mp jk_0 n_0 \Delta z \quad (11.1)$$

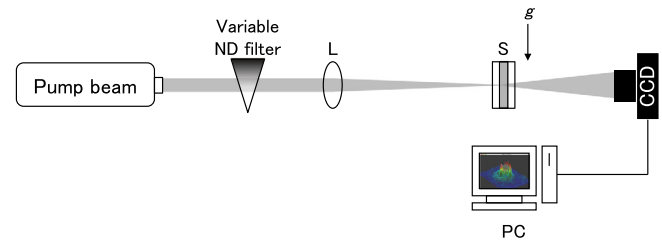
$$\gamma = k_0^2 \Delta x \Delta y [n^2(x, y, z) - n_0^2] - 4 \quad (11.2)$$

Thus the electric field is found by solving this pentadiagonal equation. Consequently, the intensity of the propagating beam can be calculated by following equation:

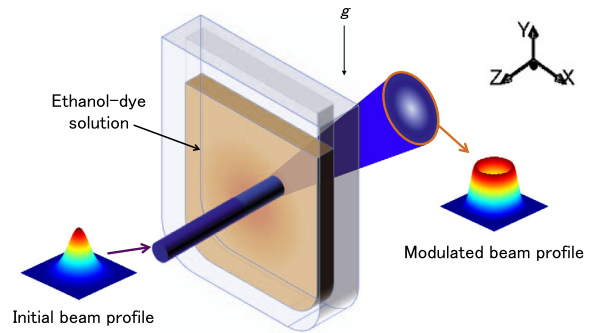
$$I(x, y, z) = |\Psi(x, y, z)|^2 \quad (12)$$

### 3. Experimental setup

Fig. 3 shows the schematic illustration of experimental apparatus. Note that the pump and probe beams are not separated as shown in Fig. 1, and only a single beam is used. As the purpose of this experiment is to verify the numerical model described in Section 2, we used only the single beam system here. An ion laser, of which wavelength is 488 nm, was used. The dye called sunset-yellow has significant absorption spectra at the wavelength of the laser [11]. In the experimental system represented in Fig. 3, some of the beam is absorbed in liquid sample to induce the thermal lens effect, and the transmitting beam experiences defocusing effect. The focal length of the lens was 240 mm, and the beam



(a) Experimental apparatus



(b) Configuration of the fluidic optical device

Fig. 3. Schematic illustration of the single beam thermal lens system: thermal self-action of the single beam was investigated.

radius at focus was 190  $\mu\text{m}$ . The cuvette of 1 mm optical thickness was set on the focal point of the beam. As the beam is narrowed in the cuvette, crucial refractive index field is formed around the beam. As a result, the transmitted beam profile is significantly modulated from the Gaussian profile to the annular-like profile as shown in Fig. 3(b). The modulated intensity profile is detected by the CCD camera and received by PC. The pump beam power was manipulated by variable ND filter from 2.0 mW to 14.0 mW. As the temperature increases only few degrees of Kelvin in the cuvette, vaporization of the liquid sample does not have to be considered. Experimental conditions are tabulated in Table 2. All the measurements are conducted in the steady state regime.

## 4. Results and discussion

### 4.1. Distortion of the beam induced by natural convection

Fig. 4 shows the intensity distributions on  $y$ -axis of the 70 mm propagated beam after the cuvette. Vertical axis and horizontal axis indicate normalized intensity and  $y$ -position respectively. Numerical results show good agreement with experimental results when natural convection takes place. The beam experienced defocusing effect to hold two large peaks as the annular-like beam. However, existence of natural convection slants the intensity profile to the direction of gravity acceleration, and a good annular-like

Table 2  
Experimental conditions.

Parameter	Unit	Value
Wavelength, $\lambda_e$	nm	488
Original beam radius, $r_0$	mm	0.4
Pump beam power, $P_0$	mW	2.0–14.0
Beam quality factor, $M^2$		<1.02
Cuvette thickness, $L$	mm	1
Absorption coefficient of the liquid sample, $\alpha$	$\text{cm}^{-1}$	1.65
Focal length of the lens, $f$	mm	240

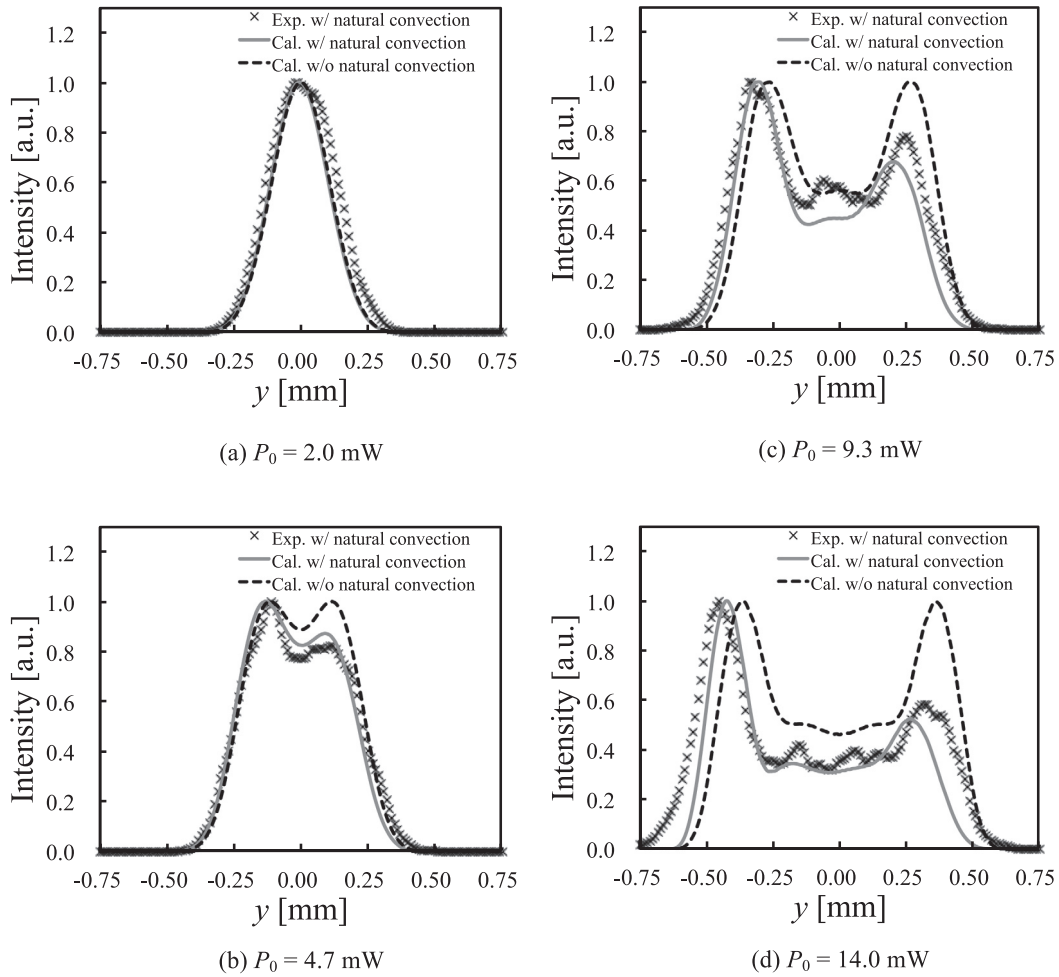
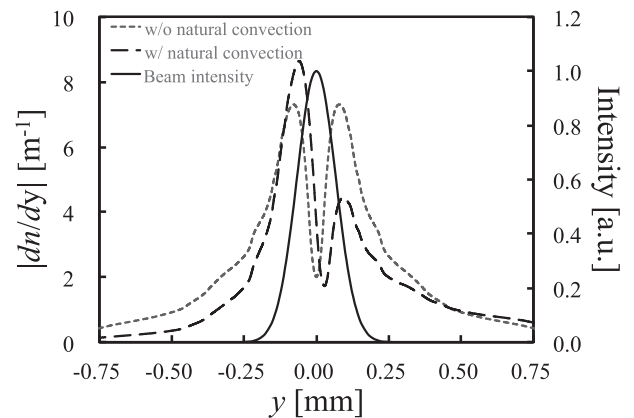


**Fig. 4.** Shaped intensity distribution: (a)  $P_0 = 2.0$  mW, (b)  $P_0 = 4.7$  mW, (c)  $P_0 = 9.3$  mW, (d)  $P_0 = 14.0$  mW. Experimental results with natural convection (cross mark), and calculated results with and without natural convection (solid line and dotted line, respectively) are indicated in each figure. The numerical model well represents modulation and distortion of the beam affected by natural convection.

beam is difficult to be obtained. The distortion becomes more obvious as input power gets larger.

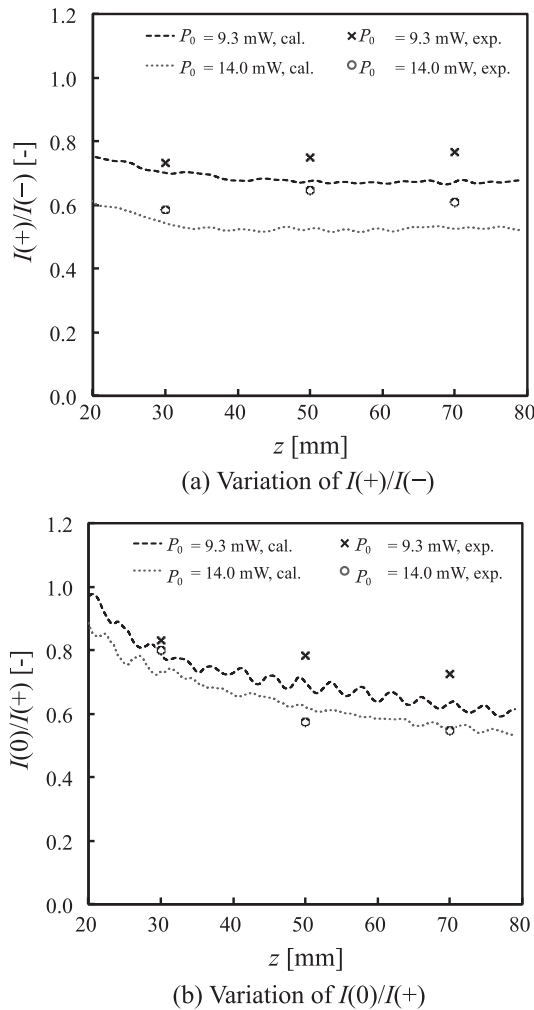
With respect to the error, several reasons (such as the original beam quality, use of the thermal properties (see Section 2.2), and axial effect in the cuvette) can be considered. However, as we set calculation conditions based on measurements (such as beam radius and focal length of the lens) and reflected beam quality factor, the effect of original beam quality could be minimized. Also, as the solution was very dilute in our experiment, it can be considered that the errors coming from the thermal properties are not crucial. Thus, axial effect in the cuvette is considered as the most influential factor of the error. Although the pump beam radius along the cuvette was set constant in Eq. (4), it is enlarged up to 3% at the exit of the cuvette due to the thermal lens effect. It results in geometrical disagreement between the pump beam and the probe beam although it is single beam system. Thus, large input power leads to the crucial error in radial direction.

Fig. 5 represents relation between the absolute value of radial refractive index gradient and the intensity distribution of the beam on  $y$ -axis. Compared to the refractive index gradient without the convection, the refractive index gradient with the convection indicates significant asymmetry around  $y = 0$  mm. In addition, refractive index field was formed much widely in radial direction compared to beam waist. For this reason, considerable beam shaping cannot be obtained by the single beam system. Therefore, separation of the probe beam is essential to take advantage of the significant refractive index field in radial direction.



**Fig. 5.** Size of the refractive index gradient and the beam intensity in the cuvette:  $P_0 = 14.0$  mW. Dotted line and dashed line indicate size of the refractive index gradient with and without natural convection respectively. Solid line indicates the beam intensity profile. Figure well demonstrates the influence of the convective flow in terms of the refractive index field that propagating beam experiences.

When  $P_0 = 9.3$  mW and  $P_0 = 14.0$  mW, two noticeable peaks are observed around the edge of the beam (see Fig. 4(c) and (d)). Here, two new parameters  $I(+)/I(-)$  and  $I(0)/I(+)$  were defined to evaluate asymmetry and quality of the annular beam. Where  $I(+)$  is the peak



**Fig. 6.** Asymmetry of the beam along propagating direction: (a) variation of  $I(+)/I(-)$ , (b) variation of  $I(0)/I(+)$ . Dashed, and dotted lines indicate calculation data of  $P_0 = 9.3$  mW, and  $P_0 = 14.0$  mW respectively. Experimental data of the indicated cases are represented as cross mark, and circle. These parameters can be used for the evaluation of the annular-like beam shaped by fluidic optical device.

intensity in the range of  $y > 0$ ,  $I(-)$  is the peak intensity in the range of  $y < 0$ , and  $I(0)$  is center intensity.  $I(+)/I(-)$  equals to 1 when natural convection does not take place, and small  $I(+)/I(-)$  indicates considerable asymmetry of the beam. On the other hand, small  $I(0)/I(+)$  indicates good quality of the annular-like beam with relatively small center intensity. Therefore, the symmetry and quality of annular beam can be investigated using two parameters. Fig. 6 demonstrates the variation of  $I(+)/I(-)$  and  $I(0)/I(+)$  along the propagation direction. As input power increases, asymmetry between two peaks becomes significant in Fig. 6(a). Asymmetry of the beam related to  $z$  and  $P_0$  was well expressed by this parameter. For the beam with propagated distance over 30 mm,  $I(+)/I(-)$  no longer decreases significantly. Rather the experimental error becomes apparent. In Fig. 6(b), center intensity decreases with large input power as propagating to  $z$  direction. No large difference between experimental and calculated result was found. Thus, asymmetry and quality of an annular-like beam in the dual beam system is to be investigated using these parameters in next section.

#### 4.2. Parametric study in dual beam system

Taking advantage of the numerical model, we performed parametric study on the influence of natural convection in the dual

**Table 3**  
Calculation conditions.

Parameter	Unit	Value
Wavelength of probe beam, $\lambda_p$	nm	1064
Original probe beam radius, $R_0$	mm	1.0
Pump beam power, $P_0$	mW	9.3
Beam quality factor, $M^2$		1.00
Focal length of the lens 2, $f$	mm	240
$z$ position of the lens 2	mm	-60, -30, 0, 30, 60

**Table 4**  
Variable parameters.

$z$ position of the lens 2 (mm)	Probe beam radius in the cuvette ( $\mu\text{m}$ )	Pump radius in the cuvette, $w_0$ ( $\mu\text{m}$ )
-60	263	
-30	149	
0	81	95
30	149	
60	263	

beam thermal lens system shown in Fig. 1. As demonstrated in Fig. 5, there is large difference between the beam size and the area where the significant refractive index field is formed in the single beam system. Thus the probe beam radius was changed primarily. Beam radius of the focused beam is written as following equation:

$$W(z) = W_0 \left[ 1 + \left( \frac{z}{z_R} \right)^2 \right]^{1/2} \quad (13)$$

where

$$W_0 = \frac{M^2 f \lambda}{\pi r_0} \quad (13.1)$$

$$z_R = \frac{\pi W_0^2}{\lambda} \quad (13.2)$$

Considering implementation of optical system, the probe beam radius was changed by the several controllable parameters such as original beam radius, and  $z$ -position of the lens 2. Calculation conditions are tabulated in Table 3. Except for the pump beam power, the pump beam parameters and the sample parameters were not changed from Table 2 for the straightforward comparison with the result of single beam system in Section 4.1. The pump beam

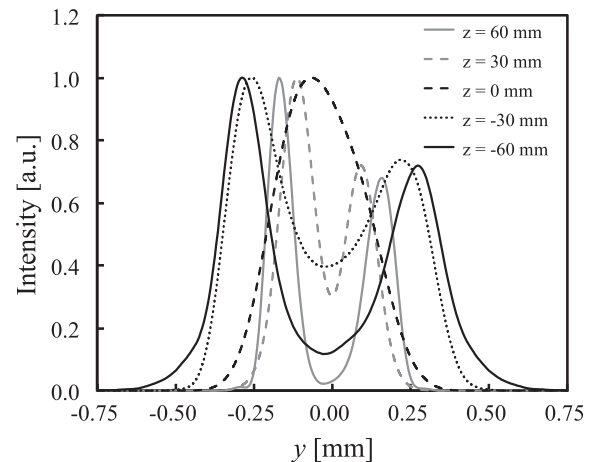


**Fig. 7.** Shaped intensity distribution: Gray solid line, dashed line, black dashed line, dotted line, and solid line indicate the beam profile when  $z$  position of the lens 2 is 60 mm, 30 mm, 0 mm, -30 mm, and -60 mm respectively. The shaped beam profile depends heavily on radius and phase of the probe beam in the cuvette.

**Table 5**  
Variation of  $I(+)/I(-)$  and  $I(0)/I(+)$  associated with shift of optical axis.

Shift ( $\mu\text{m}$ )	$I(+)/I(-)$	$I(0)/I(+)$
0 (Single/pump beam)	0.70	0.79
0	0.72	0.17
5	0.77	0.16
10	0.84	0.16
15	0.90	0.15
20	0.97	0.15
25	1.05	0.15

power was selected as 9.3 mW because the intensity distribution of the beam represented in Fig. 4(c) has the annular-like profile with less asymmetry compared to the case of  $P_0 = 14.0$  mW represented in Fig. 4(d). Changing  $z$ -position of the lens 2 leads to difference in the focal point between the two beams and variation of the probe beam radius in the cuvette. When the  $z$  position of the lens 2 is 0 mm, the focal points of the two beams coincide. This relation is tabulated in Table 4.

Fig. 7 shows the calculated beam profiles after 30 mm of the cuvette. Intensity of the beam center decreased significantly, and the annular-like profile was obtained. When  $z = 0$  mm, it is considered that the probe beam radius in the cuvette is too small to experience refractive index field and shaped into the annular-like

profile (see Table 4). Also, the beam was spread widely in radial direction when the  $z$  position is negative value. In these cases, the probe beam with spreading phase enters the cuvette as it is set after the focal point of probe beam. Therefore, we can conclude that spreading beam with relatively large radius is modulated significantly into the annular-like beam.

When  $z = 60$  mm, the parameters are  $I(+)/I(-) = 0.718$ , and  $I(0)/I(+)=0.167$ . Compared to the single beam system,  $I(0)/I(+)$  decreased considerably but  $I(+)/I(-)$  was not improved. Here, shift of the optical axis of the probe beam is taken into account as refractive index field is also shifted from optical axis as shown in Fig. 7. We shifted the optical axis of probe beam to  $y$  direction by  $5 \mu\text{m}$  increment, which is a feasible pitch for a real optical system. Table 5 indicates values of  $I(+)/I(-)$  and  $I(0)/I(+)$  of the axis-shifted beams. Fig. 8 represents the cross sectional beam profile and intensity distribution on  $y$  axis of the several beams indicated in Table 5. The comparison with the single beam system, which is used for the pump beam in the present context, is given in Table 5 and Fig. 8. As the optical axis gets shifted,  $I(+)/I(-)$  is obtained as a value close to 1. In particular,  $I(+)/I(-)$  and  $I(0)/I(+)$  were improved remarkably with  $20 \mu\text{m}$  shift. For larger than  $20 \mu\text{m}$  shift, the beam gets too isolated from the pump beam axis so that  $I(+)$  becomes larger than  $I(-)$ . The annular-like profile with  $20 \mu\text{m}$  shift in Fig. 8 also confirms that the well-shaped annular-like beam can be modulated

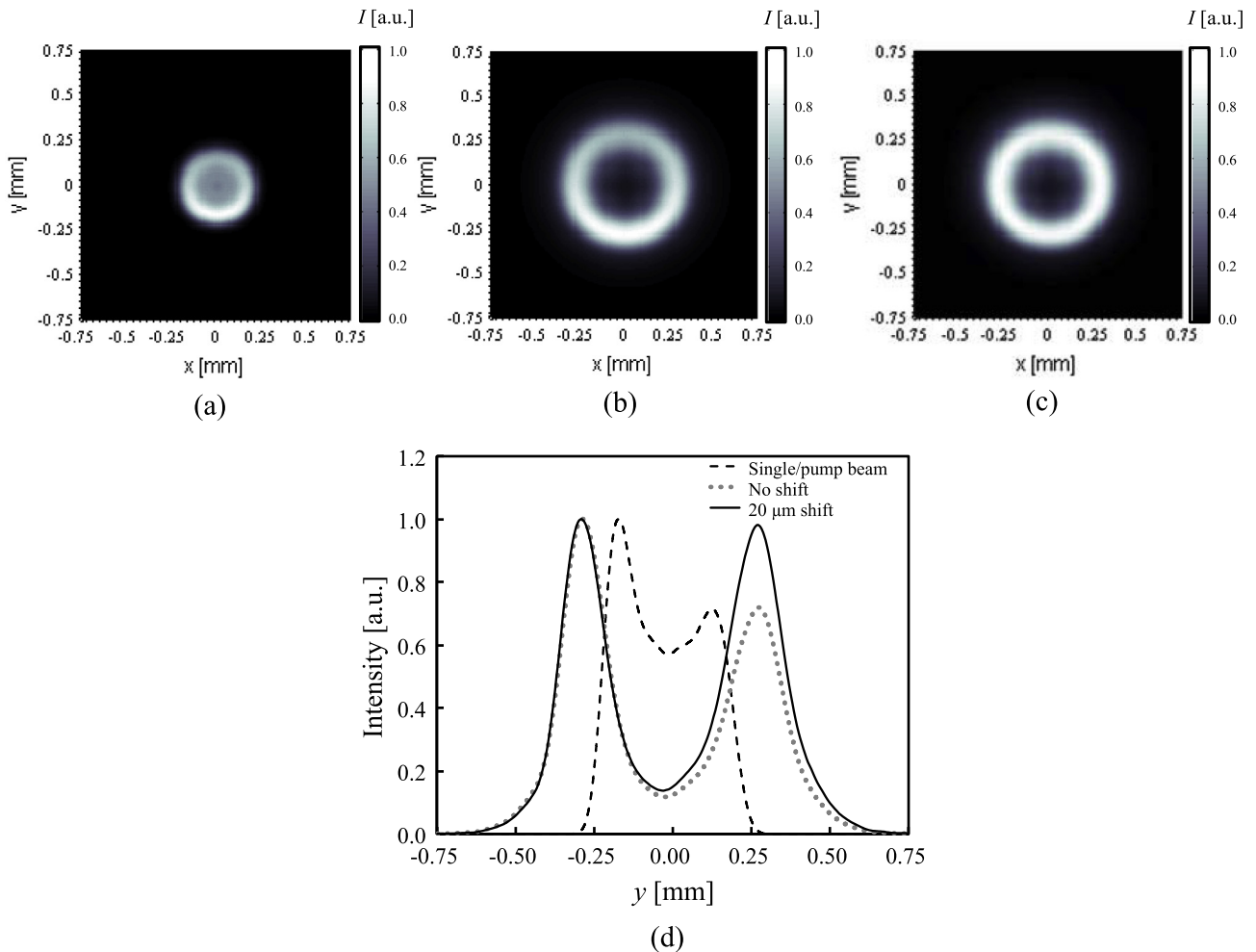


**Fig. 8.** Shaped beam profiles associated with shift of optical axis: (a)–(c) show cross sectional profile of the beams after 30 mm of the cuvette. (a) Single beam system (pump beam in the dual beam experiment), (b) dual beam system without shift of optical axis, (c) dual beam system with  $20 \mu\text{m}$  shift of optical axis. (d) Intensity distribution of the beams (a)–(c) on  $y$  axis. Dashed line, dotted line, and solid line indicate the intensity distribution of (a)–(c) in order. Well-shaped annular beam with symmetry can be obtained by adjusting optical axis.

by dual beam thermal lens system with adjustment of optical axis although natural convection takes place.

## 5. Conclusion

The influence of natural convection on beam shaping using fluidic optical device was investigated theoretically and experimentally. Beam propagation method using Padé approximant operators provided great prediction on the beam profile change. We investigated the beam profile change affected by natural convection in the fluidic optical device using this numerical method on the dual beam thermal lens system to control asymmetry caused by natural convection and to advance quality of the annular-like beam. Consequently, the well-shaped annular-like beam could be obtained by adjusting several feasible parameters (focal points difference between the two beams, beam size, and shift of optical axis) as avoiding asymmetry. It is expected that the numerical method described in this study can be used as a great tool to predict the influence of natural convection and design the thermal lens systems.

## Conflict of interest

None declared.

## Acknowledgments

Part of this work has been supported by Grant-in-Aid from JSPS/MEXT and Amada Foundation. H.D. Doan appreciates the support from JSPS.

## References

- [1] J.P. Gordon, R.C.C. Leite, R.S. Moore, S.P.S. Porto, J.R. Whinnery, Long-transient effects in lasers with inserted liquid samples, *J. Appl. Phys.* 36 (1) (1965) 3–8.
- [2] C. Hu, J.R. Whinnery, New thermo-optical measurement method and a comparison with other methods, *Appl. Opt.* 12 (1) (1973) 72–79.
- [3] J.R. Whinnery, Laser measurement of optical absorption in liquids, *Acc. Chem. Res.* 7 (7) (1974) 225–231.
- [4] S.J. Sheldon, L.V. Knight, J.M. Thorne, Laser-induced thermal lens effect: a new theoretical model, *Appl. Opt.* 21 (9) (1982) 1663–1669.
- [5] J. Shen, R.D. Lowe, R.D. Snook, A model for CW laser induced mode-mismatched dual-beam thermal lens spectrometry, *Chem. Phys.* 165 (2–3) (1992) 385–396.
- [6] M. Sheik-bahae, A.A. Said, E.W.V. Stryland, High-sensitivity, single-beam  $n_2$  measurements, *Opt. Lett.* 14 (17) (1989) 955–957.
- [7] M. Sheik-bahae, A.A. Said, T.-H. Wei, D.J. Hagan, E.W.V. Stryland, Sensitive measurement of optical nonlinearities using a single beam, *J. Quant. Electron.* 26 (4) (1990) 760–769.
- [8] P. Brochard, V. Grolier-Mazza, Thermal nonlinear refraction in dye solutions: a study of the transient regime, *J. Opt. Soc. Am. B* 14 (2) (1997) 405–414.
- [9] D.I. Kovsh, S. Yang, D.J. Hagan, E.W.V. Stryland, Nonlinear optical beam propagation for optical limiting, *Appl. Opt.* 38 (24) (1999) 5168–5180.
- [10] S.S. Yang, T.H. Wei, T.H. Huang, Y.C. Chang, Z-scan study of thermal nonlinearities in silicon naphthalocyanine-toluene solution with the excitations of the picosecond pulse train and nanosecond pulse, *Opt. Express* 15 (4) (2007) 1718–1731.
- [11] H.D. Doan, Y. Akamine, K. Fushinobu, Fluidic laser beam shaper by using thermal lens effect, *Int. J. Heat Mass Transfer* 55 (11–12) (2012) 2807–2812.
- [12] H.D. Doan, Y. Akamine, N. Iwatani, M. Kohno, K. Fushinobu, Generation of Bessel beam by using thermal lens effect, *Trans. Jpn. Soc. Mech. Eng. (in Japanese)* 79 (803) (2013) 1354–1362.
- [13] B. Kim, R. Inoue, H.D. Doan, K. Fushinobu, Pulse-shaping of nanosecond pulse laser by means of thermal lens effect, *Trans. Jpn. Soc. Mech. Eng. (in Japanese)* 80 (815) (2014).
- [14] S.A. Akhmanov, D.P. Krindach, A.V. Migulin, A.P. Sukhorukov, R.V. Khokhlov, Thermal self-actions of laser beam, *J. Quant. Electron.* 4 (10) (1968) 568–575.
- [15] R.D. Boyd, C.M. Vest, Onset of convection due to horizontal laser beams, *Appl. Phys. Lett.* 26 (6) (1975) 287–288.
- [16] S.S. Sarkisov, Circulation of fluids induced by self-acting laser beam, *J. Appl. Phys.* 99 (2006) 114903.
- [17] R. Karimzadeh, Spatial self-phase modulation of a laser beam propagating through liquids with self-induced natural convection flow, *J. Opt.* 14 (2012) 095701.
- [18] K. Kitamura, K. Sakai, S. Noda, Sub-wavelength focal spot with long depth of focus generated by radially polarized, narrow-width annular beam, *Opt. Express* 18 (5) (2010) 4518–4525.
- [19] I.G. Cormack, M. Mazilu, K. Dholakia, C.S. Herrington, Fluorescence suppression within Raman spectroscopy using annular beam excitation, *Appl. Phys. Lett.* 91 (2007) 023903.
- [20] The Japan Society of Mechanical Engineers ed., *JSPS Data Book: Heat Transfer*, The Japan Society of Mechanical Engineers (in Japanese), 1986, p. 350.
- [21] J.V. Roey, J.V.D. Donk, P.E. Lagasse, Beam-propagation method: analysis and assessment, *J. Opt. Soc. Am.* 71 (7) (1981) 803–810.
- [22] G.R. Hadley, Wide-angle beam propagation using Padé approximant operators, *Opt. Lett.* 17 (20) (1992) 1426–1428.